MEASUREMENT OF THE LAMB SHIFT IN HELIUMLIKE URANIUM (U^{90+})

Harvey Gould and Charles T. Munger

Materials and Molecular Research Division, Building 71–259
Lawrence Berkeley Laboratory, University of California,
Berkeley California 94720 U.S.A.

DISCLAIMER

MEASUREMENT OF THE LAMB SHIFT IN HELIUMLIKE URANIUM (U^{90+})

Harvey Gould and Charles T. Munger

Materials and Molecular Research Division, Building 71-259
Lawrence Berkeley Laboratory, University of California,
Berkeley California 94720 U.S.A.*

1. INTRODUCTION

The production[1] in 1983 of a beam of bare U^{92+} at the Lawrence Berkeley Laboratory's Bevalac[2], the Bevatron and Super-HILAC operating in tandem, demonstrated the feasibility of experiments using few-electron uranium. In 1984 x rays from radiative electron capture into the K shell of uranium was observed[3,4] by Anholt et. al., and in the same year x rays from n = 2 → n = 1 transitions in hydrogenlike uranium (U^{91+}) and heliumlike uranium (U^{90+}) were observed by Munger and Gould[5]. This article discusses our recent measurement of the Lamb shift in heliumlike uranium[6]. Our value of 70.4 (8.1) eV for the one-electron Lamb shift in uranium is in agreement with the theoretical value[7,8] of 75.3 (0.4) eV.

2. QUANTUM ELECTRODYNAMICS AT Z = 92

A possible failure of quantum electrodynamics (QED) to predict accurate radiative corrections to bound states at Z = 92 is not ruled out by its success at low Z. The largest contribution to the Lamb shift at Z = 92 comes from terms in the electron self-energy[9] which are high powers of $Z\alpha$ and which are invisible in experiments at low Z. Lamb shift measurements on high-Z electronic and muonic atoms are complementary because muonic atom measurements are sensitive to higher order vacuum polarization effects but not to self-energy effects[10].

The contribution of the higher order terms in the self-energy can be seen by comparing the series expansion of the self energy with an evaluation[7] of the self-energy to all orders in $Z\alpha$. If we write the self energy Σ_n in a power series in α and $Z\alpha$, we have:

$$\Sigma_n = n^{-3}(\alpha/\pi) m_o c^2 \left[|A_{40} + A_{41} ln(Z\alpha)^{-2}|(Z\alpha)^4 + A_{50}(Z\alpha)^5 \right.$$
$$+ |A_{60} + A_{61} ln(Z\alpha)^{-2} + A_{62} ln^2(Z\alpha)^{-2}|(Z\alpha)^6 + A_{70}(Z\alpha)^7 \quad (1)$$
$$\left. + \text{higher order terms} \right]$$

Where n is the principal quantum number and m_o is the electron rest mass. Values of the coefficients $A_{40} - A_{70}$ can be found in Ref. 9. Figure 1 shows the ratio of the higher order terms in the self-energy to

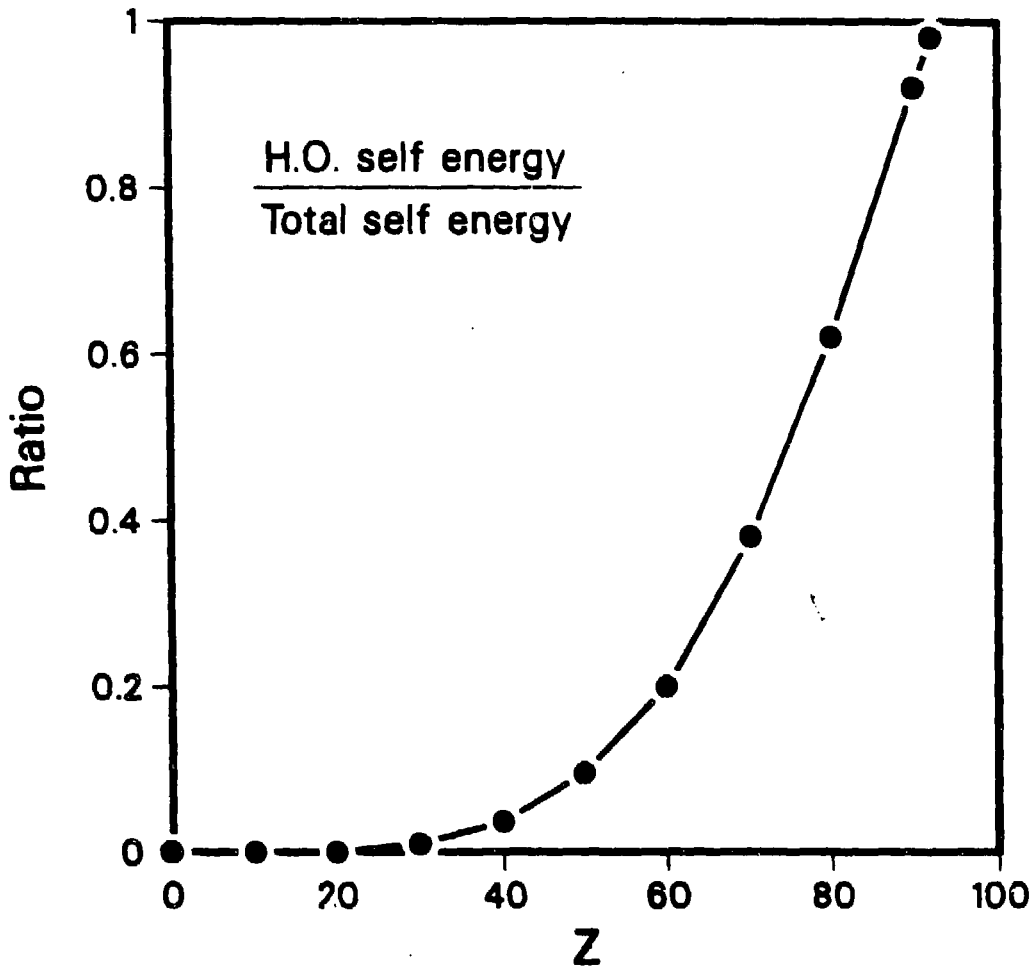$$\frac{\text{H.O. self energy}}{\text{Total self energy}}$$

FIGURE 1

Ratio of the higher order terms in the self-energy to the total self-energy obtained by comparing the series expansion value through term A_{70} $(Z\ \alpha)^7$ with a numerical calculation to all orders in $Z\alpha$.

the total self energy. In neutral hydrogen the higher order terms in the self-energy are negligible but at Z = 92 they are the largest contribution to the Lamb shift.

3. LAMB SHIFT MEASUREMENT AT Z = 92

3.1 Experimental Technique

Our measured value of 70.4 (8.1) eV for the one-electron Lamb shift in uranium it is in agreement with the theoretical value[7,8] of 75.3 (0.4) eV based upon a calculation of the self-energy by Mohr[7]. We extract our Lamb shift from our beam-foil time-of-flight measurement of 54.4 (3.3) ps for the lifetime of the 2 $^3P_0$ state of heliumlike uranium.

The 2 $^3P_0$ state (Fig. 2) is the only low-lying excited state found in hydrogenlike uranium or heliumlike uranium whose long lifetime allows its decay to be observed in vacuum downstream from the target
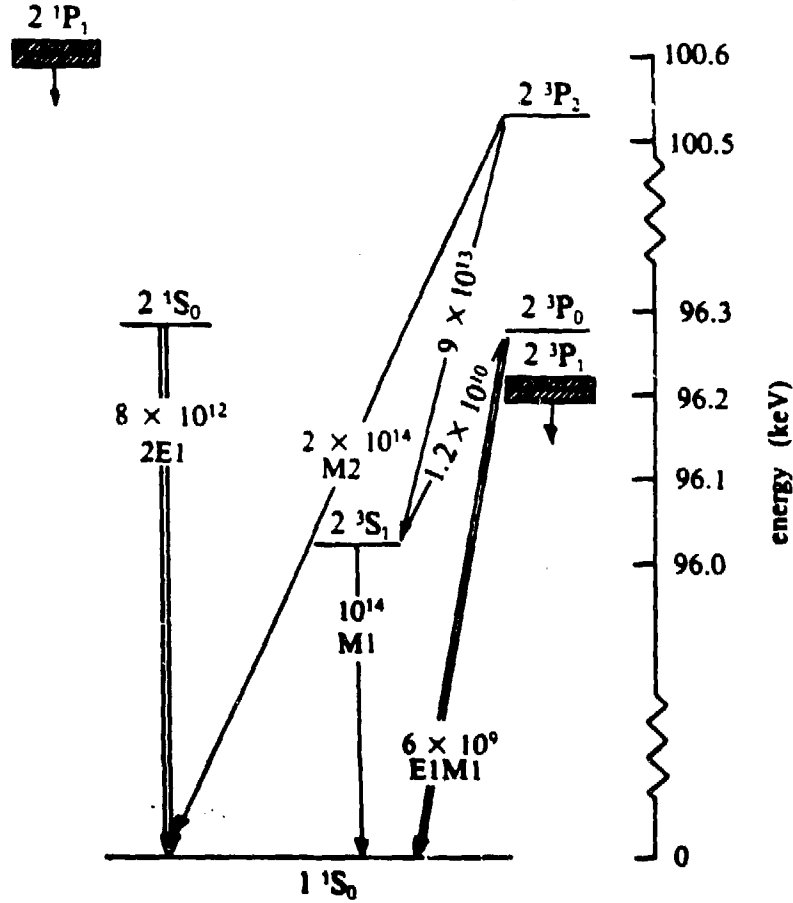
Heliumlike Uranium

FIGURE 2
Energy level diagram of the n = 1 and n = 2 states of heliumlike uranium.
Decay rates, except for the 2 $^3P_0$ state, are taken from Ref. 13. Energies
are taken from Refs. 7, 8, and 13. M1 and M2 decays are magnetic-dipole
and magnetic-quadrupole decays, respectively, and decays without labels
are electric-dipole decays. An approximate radiative width is indicated for
the $^1P_1$ and $^3P_1$ states.

in which it is produced. In heliumlike uranium the 2 $^3P_0$ state decays 70% of the time to the 2 $^3S_1$ state by
an electric-dipole (E1) transition. This makes the 2 $^3P_0$ lifetime sensitive to the 2 $^3P_0$ - 2 $^3S_1$ energy differ-
ence of 260.0 (7.8) eV (experimental value) and hence to the Lamb shift. At Z = 92 the major contribu-
tions to the calculated Lamb shift are the self-energy[7] of 56.7 eV, the leading order term in the vacuum
polarization[7,8] of −14.3 eV and the finite nuclear size correction[8] of 32.5 eV. In heliumlike uranium there
is also a small screening correction to the radiative corrections — expected to be of order 1/Z times the
self-energy[10,11]. For zero Lamb shift the 2 $^3P_0$ − 2 $^3S_1$ states would be split by the difference in the $1s_{1/2}$
− $2s_{1/2}$ and $1s_{1/2}$ − $2p_{1/2}$ Coulomb interactions. This splitting at Z = 92 has been calculated by Mohr[12]
to be 330.4 eV, which agrees (1 eV) with the calculations of Lin, Johnson and Dalgarno[13] and of Drake[14].
The other significant decay of the 2 $^3P_0$ state is to the 1 $^1S_0$ ground state by a two-photon electric-dipole

magnetic-dipole (E1M1) transition[14]. To obtain the Lamb shift we combine our measured $2\,^3P_0$ lifetime and the calculated values for the E1M1 decay rate[14], the $2\,^3P_0 - 2\,^3S_1$ E1 matrix element[15], and the $2\,^3P_0 - 2\,^3S_1$ Coulomb splitting[12].

3.2 Production of the $2\,^3P_0$ State of Heiumlike Uranium

Few-electron uranium and other very high-Z ions are produced by stripping relativistic ions[1]. Relativistic ions through uranium at energies of up to 1000 MeV/amu are obtained at the Lawrence Berkeley Laboratory's Bevalac[2]. The experimentally determined charge state distributions for relativistic uranium ions which have passed through equilibrium thickness targets (typically a few ten's of mg/cm^2 for high-Z targets) is shown in Fig. 3. The processes for electron capture and loss by relativistic heavy ions are well understood and cross sections for ionization, for radiative electron capture and for nonradiative electron capture can be reliably calculated[16-18].

Heliumlike uranium in the $2\,^3P_0$ state is prepared by capture of an electron in a foil by hydrogenlike uranium The hydrogenlike uranium is made by stripping a beam of 220 MeV/amu uranium 39+ in an equilibrium thickness target. An aluminum target produces an equilibrium charge state distribution of roughly 5% U92+, 30% U91+, 60% U90+, and 5% U89+. The hydrogenlike U91+ fraction is magnetically selected and transported to a 0.9 mg/cm^2 Pd foil. In the Pd foil about half of the U91+ ions are converted to heliumlike U90+, with about 1% of these being formed in the $2\,^3P_0$ state or in states which rapidly decay to the $2\,^3P_0$ state.

3.3 Decay of the $2\,^3P_0$ State

Downstream from the Pd foil we observe, not the 260 eV photon from the $2\,^3P_0 \rightarrow 2\,^3S_1$ transition, but instead the 96.01 keV x ray from the subsequent fast decay of the $2\,^3S_1$ state to the $1\,^1S_0$ ground state. The 96.01 keV x ray is much easier to detect than the 260 eV photon, and the $2\,^3S_1$ lifetime[13] of 10^{-14} s has no effect on the measured $2\,^3P_0$ lifetime provided sufficient time is allowed for the initial $2\,^3S_1$ population to decay.

Figure 4 shows a spectrum recorded by one of our Ge x-ray detectors collimated to view emission perpendicular to the uranium beam at a point 0.67 cm downstream from the Pd foil. The 96.01 keV x ray from the $2\,^3P_0$-fed $2\,^3S_1 \rightarrow 1\,^1S_0$ decay is Doppler shifted and appears as a peak at 77.76 (0.18) keV. We identified this peak by its correct transverse Doppler shift and exponential decay at two different beam energies, 218 MeV/amu and 175 MeV/amu (here determined from the operating conditions of the Bevalac and corrected for energy loss in foils); by the dependence of the Doppler broadened peak width on the angular acceptance of the detector; by the yield[16,17] using foils of different Z and thickness; by the peak's absence when the foil is removed; and by the lack of any other long-lived, low-lying states of heliumlike uranium or hydrogenlike uranium besides the $2\,^3P_0$ state.

The height of the peak above background was found by a maximum-likelihood fit of a quadratic to the background. The decay curve (Fig. 5), which spans 2.7 decay lengths, is a maximum-likelihood fit of a single exponential to the data. The reduced χ^2 for the fit is 0.89. The spectrum shown in Fig. 4 contributes to the first point at 0.67 cm in Fig. 5. The 1/e decay length is 1.182 (0.069) cm, and the 5.8% statistical error dominates our final error in the $2\,^3P_0$ lifetime. Other contributions to our 6.2% total lifetime
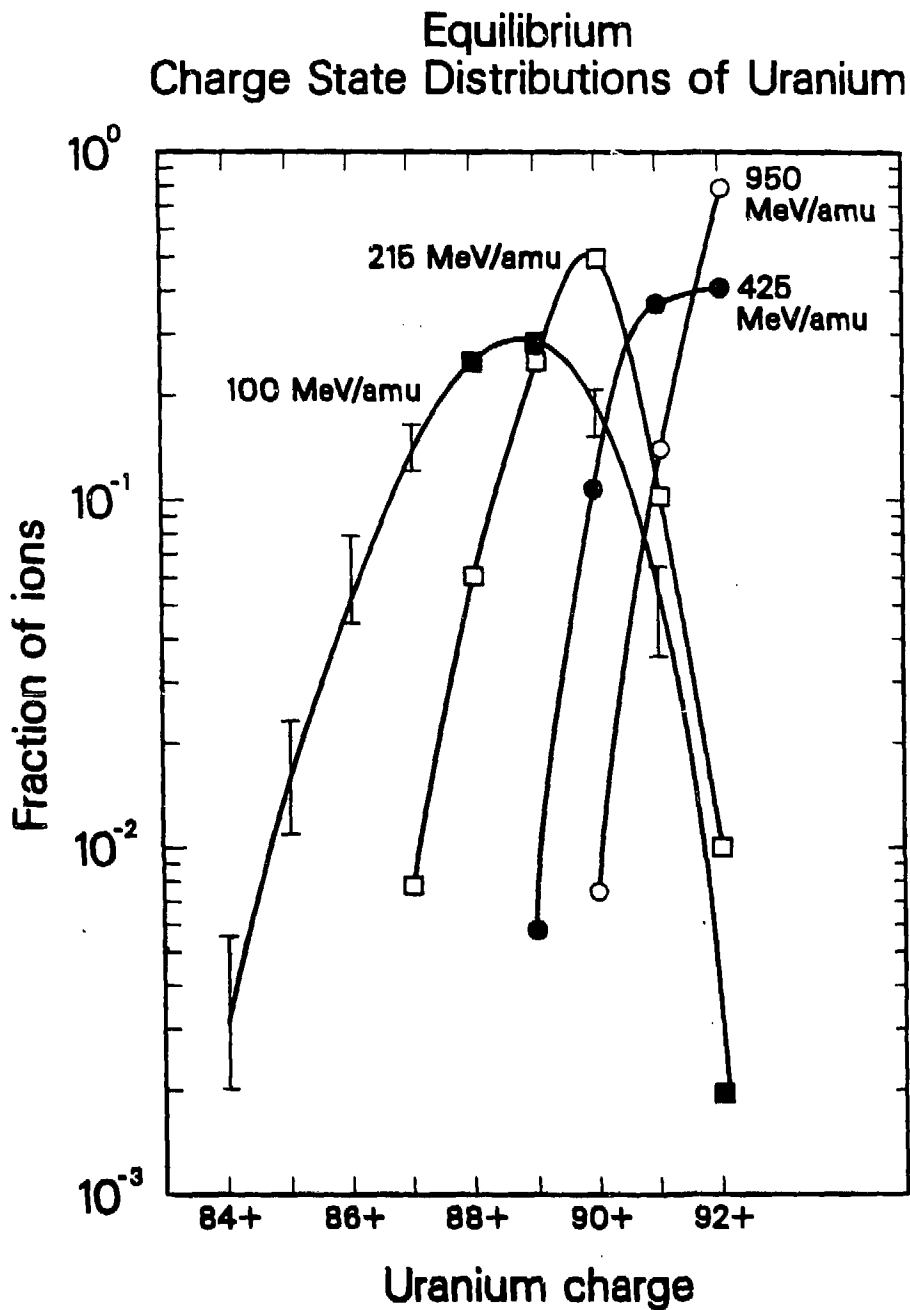
Equilibrium
Charge State Distributions of Uranium

FIGURE 3

Charge state distribution of relativistic uranium after passing through an equilibrium thickness target. A Cu (Z = 29) target was used for the 950 MeV/amu, 425 amu, and 100 MeV/amu uranium. A Au (Z = 79) target was used for the 215 MeV/amu uranium. Data are from Ref. 18.

error are: 1.2% from the determination of the beam velocity and time dilation using the transverse Doppler shift of the $2\,^3S_1 \rightarrow 1\,^1S_0$ transition and 1.8% from the experimental upper limit to contamination of our signal by cascade feeding. Our value for the $2\,^3P_0$ lifetime is 54.4 (3.3)ps.
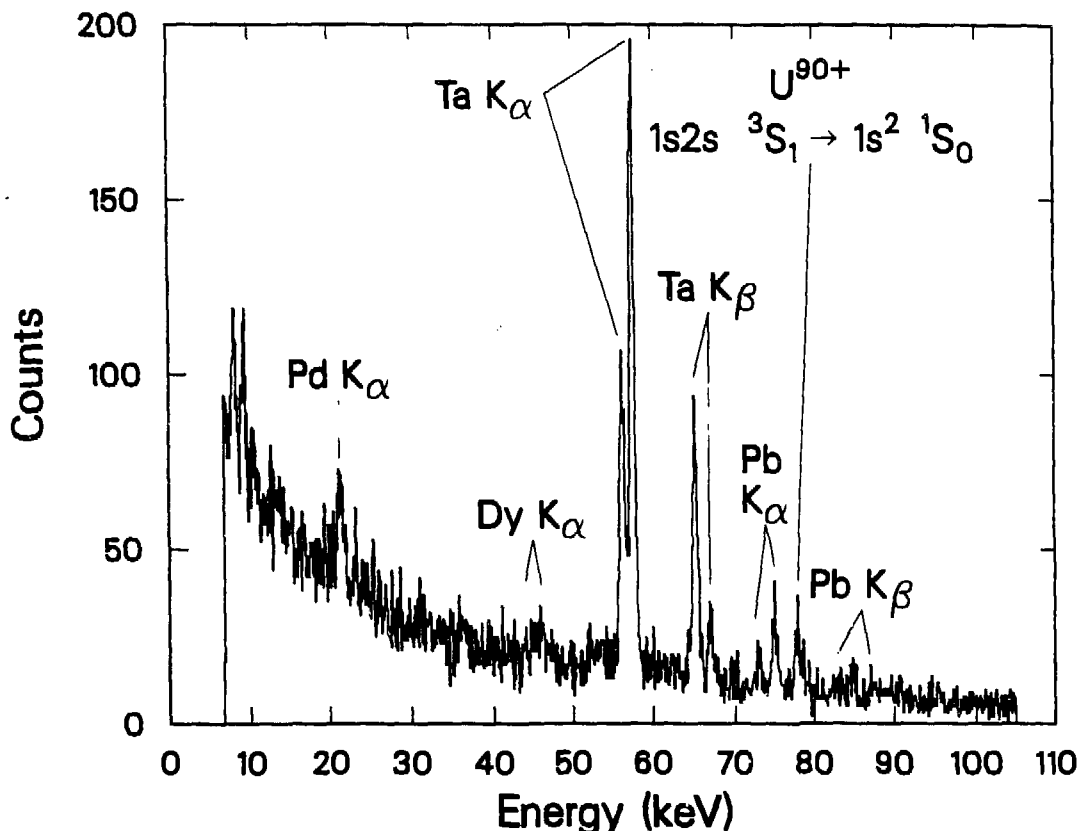
FIGURE 4

Spectrum recorded by a Ge x-ray detector collimated to view emission perpendicular to the uranium beam at a point 0.67 cm downstream from the Pd foil. This spectrum represents 135 minutes of counting — about 10^8 uranium ions. The Doppler-shifted peak from the decay of $2\ {}^3P_0 \to 2\ {}^3S_1 \to 1\ {}^1S_0$ is at 77.8 keV. Cascades from higher excited states would produce a peak at 81.4 keV. Peaks at 72.8 keV and 75.0 keV are Pb $K_{\alpha2}$ and Pb $K_{\alpha1}$ x rays, and those at 84.5 keV–87.3 keV are Pb $K_{\beta1-\beta3}$ x rays. Peaks at 56.3 keV and 57.5 keV are Ta $K_{\alpha2}$ and Ta $K_{\alpha1}$ x rays, and those at 65.2 and 67.0 keV are Ta $K_{\beta1}$ and $K_{\beta2}$ x rays. Peaks at 45.2 keV–46.0 keV are Dy $K_{\alpha2-\alpha1}$ x rays. Pb and Dy are used for shielding and Ta is used for x-ray detector collimators. The peak at 21.2 keV is scattered Pd $K_{\alpha1}$ radiation from the Pd foil. Background is caused by bremsstrahlung of the foil electrons in the field of the uranium projectile; by bremsstrahlung of electrons scattered in and ejected from the Pd foil; and by fast nuclear fragments colliding with the Ge in the x-ray detector. Other sources of background may also exist. To reduce background we restricted the scatter of x rays into the detector, held electrons ejected from the foil away from the detector with a magnetic field, and vetoed background from nuclear fragments using scintillators.

3.4 Cascade Feeding of $2\ {}^3S_1$

A disadvantage in using the $2\ {}^3P_0$-fed $2\ {}^3S_1 \to 1\ {}^1S_0$ decay as a signal is that it makes the measured $2\ {}^3P_0$ lifetime sensitive to cascade feeding of the $2\ {}^3S_1$ state. States of heliumlike uranium with principal quantum number (n) < 22 will cascade to the $1\ {}^1S_0$ ground state before we begin our measurement of the $2\ {}^3P_0$ lifetime. Only the very small population of states with n $\geqslant$ 22 and high total angular momentum (J) can perturb our measurement by cascading down the chain of yrast states (states of J = n) to reach the $2\ {}^3P_2$ state. The $2\ {}^3P_2$ state (Fig. 2) decays 2/3 of the time to the $1\ {}^1S_0$ ground state but also decays 1/3 of the time to the $2\ {}^3S_1$ state, contaminating our $2\ {}^3S_1 \to 1\ {}^1S_0$ signal. We set a limit to this contamination
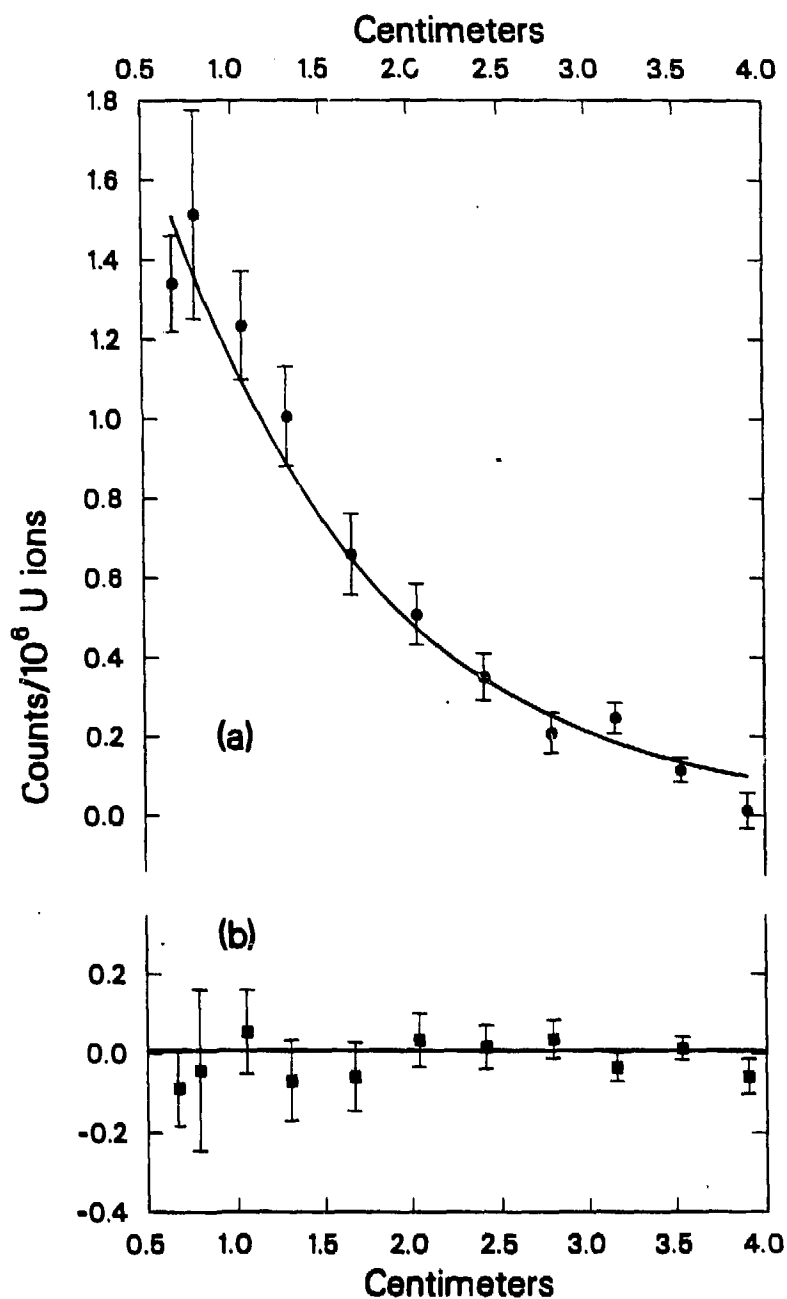
FIGURE 5

Linear plots of the intensity of x rays from the transitions (a) $2 \, ^3S_1 \rightarrow 1 \, ^1S_0$, and (b) $2 \, ^3P_2 \rightarrow 1 \, ^1S_0$, as a function of distance downstream from the Pd foil. Each point is the sum of the spectra from two x-ray detectors. Error bars are one standard deviation statistical errors. The horizontal line in (b) is the fit of a hypothetical constant count rate to the data. The count rate is consistent with zero and sets a limit to the contamination of our signal by cascade feeding.

by searching for the 100.3 keV x ray from the $2\,^3P_2 \to 1\,^1S_0$ transition, which would appear as an isolated peak Doppler shifted to 81.4 keV. The count rate in this supposed peak, after subtraction of the background, is plotted in Fig. 5. The count rate is consistent with zero with an uncertainty which contributes 1.8% to the uncertainty in the $2\,^3P_0$ decay length. Cascades from high n,J states in the hydrogenlike fraction of our beam feed the $2\,^2P_{3/2} \to 1\,^2S_{1/2}$ transition at 102.2 keV and will not interfere with our signal.

3.5 Results

From our $2\,^3P_0$ lifetime of 54.4 (3.3)ps and Drake's calculated E1M1 decay rate[14] of $0.564(5) \times 10^{10}$ s^{-1} we obtain a $2\,^3P_0 - 2\,^3S_1$ E1 decay rate of $1.273\,(0.113) \times 10^{10}\,s^{-1}$. Using the dipole length formula for the E1 decay rate[15]: $A = 12\alpha k^3\,(Z\alpha)^{-2}\,|0.792+0.759/Z|^2$ ($\hbar = m = c = 1$) we find for k, the $2\,^3P_0 - 2\,^3S_1$ splitting, a value of 260.0 (7.7) eV. Subtracting the calculated Coulomb contribution[12] of 330.4 eV yields a Lamb shift of 70.4 (7.7) eV.

So far we have accounted only for experimental uncertainty; theoretical uncertainty comes from the effect of small terms omitted from the calculations. We estimate that a $Z^{-1}\,(Z\alpha)^2$ correction to the $2\,^3P_0 - 2\,^3S_1$ E1 matrix element, and a $1/Z$ correction to the E1M1 decay rate, contribute a total of ≈ 1 eV to our inferred $2\,^3P_0 - 2\,^3S_1$ splitting; that a $Z^{-2}\,(Z\alpha)^6$ term contributes ≈ 2 eV to the 330.4 eV Coulomb splitting of the $2\,^3P_0 - 2\,^3S_1$ states; and that a $1/Z$ screening correction to the self energy, vacuum polarization and finite nuclear size contributes ≈ 1 eV to the Lamb shift. These combine to give a separate theoretical error of 2.4 eV in our extracted value of the Lamb shift.

In conclusion, we have measured the Lamb shift in uranium. Our final value of 70.4 (8.1) is in agreement with the theoretical value[7,8] of 75.3(0.4) eV.

4. FUTURE EXPERIMENTS

With more intense uranium beams and the knowledge gained from these early experiments a direct measurement of the ≈ 284 eV $2\,^2P_{1/2} - 2\,^2S_{1/2}$ splitting[19] in lithiumlike uranium (U^{89+}) to an accuracy of a few-parts in 10^4 appears feasible. When compared with atomic structure calculations of similar accuracy this would test the Lamb shift to 0.1%. The nuclear size of the uranium nucleus is well known from muonic atom measurements[21].

ACKNOWLEDGEMENTS

REFERENCES

1) H. Gould, D. Greiner, P. Lindstrom, T.J.M. Symons, and H. Crawford, Phys. Rev. Lett. 52, 180 (1984) (Errata, 52, 1654 [1984]).

2) J.R. Alonso, R.T. Avery, T. Elioff, R.J. Force, H.A. Grunder, H.D. Lancaster, J.R. Meneghetti, F.B. Selph, R.R. Stevenson, and R.B. Yord, Science 217, 1135 (1982).

3) R. Anholt, W.E. Meyerhof, Ch. Stoller, E. Morenzoni, S.A. Andriamonje, J.D. Molitoris, D.H.H. Hoffmann, H. Bowman, J.S. Xu, Z.Z. Xu and J.O. Rasmussen, Phys. Rev. Lett. 53 ,234 (1984).

4) R. Anholt, Ch. Stoller, J.D. Molitoris, D.W. Spooner, E. Morenzoni, S.A. Andriamonje, W.E. Meyerhof, H. Bowman, J.-S. Xu, Z.-Z. Xu, J.O. Rasmussen, and D.H.H. Hoffmann, Phys. Rev. A33, 2270 (1986).

5) C. Munger and H. Gould, Bull. Am. Phys. Soc. 30, 860 (1985).

6) C.T. Munger and H. Gould, submitted to Phys. Rev. Lett. (1986).

7) P.J. Mohr, Phys. Rev. Lett. 34, 1050 (1975); P.J. Mohr, Phys. Rev. A26, 2338 (1982).

8) W.R. Johnson and G. Soff, Atomic Data and Nucl. Data Tables 33, 405 (1985).

9) G.W. Erickson, Phys. Rev. Lett. 27, 780 (1971); P.J. Mohr, Ann. Phys. New York 88, 26 (1974); P.J. Mohr, private communication.

10) For a review of strong field QED, see S.J. Brodsky and P.J. Mohr, in: *Structure and Collisions of Ions and Atoms.* ed. I.A. Sellin (Springer, Berlin, 1978), Topics in Current Physics, Vol. 5, p. 3.

11) P.J. Mohr, in *Relativistic Effects in Atoms, Molecules, and Solids* edited by G.L. Malli (Plenum, New York, 1983), p. 145.

12) P.J. Mohr, Phys. Rev. A32, 1949 (1985); P.J. Mohr, in *Beam Foil Spectroscopy* edited by I.A. Sellin and D.J. Pegg (Plenum, New York, 1976), Vol 1, p. 97; P.J. Mohr, private communication.

13) C.D. Lin, W.R. Johnson, and A. Dalgarno, Phys. Rev. A15, 154 (1977); F. Parpia, and W.R. Johnson, private communication.

14) G.W.F. Drake, Nucl. Instrum. Methods in Phys. Research B9, 465 (1985); G.W.F. Drake, private communication.

15) M. Hillery and P.J. Mohr, Phys. Rev. A21, 24 (1980); H. Gould, R. Marrus, and P.J. Mohr, Phys. Rev. Lett. 33, 676 (1974).

16) W.E. Meyerhof, R. Anholt, J. Eichler, H. Gould, Ch. Munger, J. Alonso, P. Thieberger, and H.E. Wegner, Phys. Rev. A32, 3291 (1985); R. Anholt and W.E. Meyerhof, Phys. Rev A33, 1556 (1986); R. Anholt and H. Gould, Relativistic Heavy-Ion-Atom Collisions, to be published in: "Advances in Atomic and Molecular Physics," B. Bederson, ed., Academic Press, Orlando FL (1987); Lawrence Berkeley Laboratory Report No. LBL-20661.

17) J. Eichler, Phys. Rev. A32, 112 (1985); R. Anholt, and J. Eichler, Phys. Rev. A31, 3505 (1985).

18) R. Anholt, W.E. Meyerhof, X.-Y. Xu, H. Gould, B. Feinberg, R.M. McDonald, H.E. Wegner and P. Thieberger, submitted to Physical Review A.

19) K.T. Cheng, Y.-K. Kim, and J.P. Desclaux, Atomic Data and Nucl. Data Tables, 24, 111 (1979); Y.-K. Kim and J.P. Desclaux, Phys. Rev. Lett. 36, 139 (1976); see also L. Armstrong, Jr., W.R. Fielder, and D.L. Lin, Phys. Rev. A14, 1114 (1976); C. F. Fisher and T. Brage, private communication.

20) J.D. Zumbro, E.B. Shera, Y. Tanaka, C.E. Bemis, Jr., R.A. Naumann, M.V. Hoehn, W. Reuter and R.M. Steffen, Phys. Rev. Lett. 20, 1888 (1984).